Published OnlineFirst August 23, 2011; DOI:10.1158/0008-5472.CAN-11-1291

Cancer Research

# p38γ Promotes Breast Cancer Cell Motility and Metastasis through Regulation of RhoC GTPase, Cytoskeletal Architecture, and a Novel Leading Edge Behavior

Devin T. Rosenthal, Harish Iyer, Silvia Escudero, et al.

*Cancer Res* 2011;71:6338-6349. Published OnlineFirst August 23, 2011.

Published OnlineFirst August 23, 2011; DOI:10.1158/0008-5472.CAN-11-1291



Cancer Research

# p38γ Promotes Breast Cancer Cell Motility and Metastasis through Regulation of RhoC GTPase, Cytoskeletal Architecture, and a Novel Leading Edge Behavior

Devin T. Rosenthal[1,4], Harish Iyer[2], Silvia Escudero[6], Liwei Bao[1], Zhifen Wu[1], Alejandra C. Ventura[7], Celina G. Kleer[3,4,5], Ellen M. Arruda[2], Krishna Garikipati[2], and Sofia D. Merajver[1,4,5]

## Abstract

Understanding the molecular alterations that confer cancer cells with motile, metastatic properties is needed to improve patient survival. Here, we report that p38γ motogen-activated protein kinase regulates breast cancer cell motility and metastasis, in part, by controlling expression of the metastasis-associated small GTPase RhoC. This p38γ–RhoC regulatory connection was mediated by a novel mechanism of modulating RhoC ubiquitination. This relationship persisted across multiple cell lines and in clinical breast cancer specimens. Using a computational mechanical model based on the finite element method, we showed that p38γ-mediated cytoskeletal changes are sufficient to control cell motility. This model predicted novel dynamics of leading edge actin protrusions, which were experimentally verified and established to be closely related to cell shape and cytoskeletal morphology. Clinical relevance was supported by evidence that elevated expression of p38γ is associated with lower overall survival of patients with breast cancer. Taken together, our results offer a detailed characterization of how p38γ contributes to breast cancer progression. Herein we present a new mechanics-based analysis of cell motility, and report on the discovery of a leading edge behavior in motile cells to accommodate modified cytoskeletal architecture. In summary, these findings not only identify a novel mechanism for regulating RhoC expression but also advance p38γ as a candidate therapeutic target. *Cancer Res; 71(20); 6338–49. ©2011 AACR.*

### Major Findings

By combining cell biology and computational mechanical modeling, we establish p38γ as a metastasis-enabling gene responsible for controlling breast cancer cell motility. Additionally, we demonstrate how p38γ specifically exerts this effect: We show that the dynamics of leading edge actin protrusion and trailing edge retraction by stress fibers determine the type of cell motility and locomotion, but they cannot act independently of cell shape and cytoskeletal architecture. We further deduce that p38γ is the key signaling link between cell shape, cytoskeletal structure, and the type of motion the cell exhibits, and that this occurs in part through regulation of RhoC GTPase.

## Introduction

Breast cancer presents as a dysplastic disease of mammary epithelial cells, which can grow uncontrollably for years yet remain confined within mammary ducts or lobules. If diagnosed at an early stage, breast cancer responds well to therapeutic intervention (1). Breast cancer becomes much more severe once the cancer cells exit the mammary ducts and metastasize to vital organs. Understanding the molecular alterations that confer metastatic properties to otherwise benign cells is therefore essential in controlling the disease and improving patient survival.

p38 mitogen-activated protein kinase (MAPK) is a serine/threonine kinase that integrates extracellular stimuli and translates them into cellular responses by phosphorylating a network of downstream effector proteins (2). The p38 arm of

**Authors' Affiliations:** Departments of [1]Internal Medicine, [2]Mechanical Engineering, and [3]Pathology, [4]Cellular and Molecular Biology Program, and [5]University of Michigan Comprehensive Cancer Center, University of Michigan, Ann Arbor, Michigan; [6]Department of Pediatric Oncology, Dana-Farber Cancer Institute and Children's Hospital Boston, Harvard Medical School, Boston, Massachusetts; and [7]Laboratorio de Fisiología y Biología Molecular, Departamento de Fisiología, Biología Molecular y Celular, IFIBYNE-CONICET, Facultad de Ciencias Exactas y Naturales, Universidad de Buenos Aires, Buenos Aires, Argentina.

**Note:** Supplementary data for this article are available at Cancer Research Online (http://cancerres.aacrjournals.org/).

**Corresponding Author:** Sofia D. Merajver, University of Michigan Comprehensive Cancer Center, 1500 East Medical Center Drive, Room 7217, Ann Arbor, MI 48109. Phone: 734-936-6884; Fax: 734-936-7376; E-mail: smerajve@umich.edu

**doi:** 10.1158/0008-5472.CAN-11-1291

Published OnlineFirst August 23, 2011; DOI:10.1158/0008-5472.CAN-11-1291



## Quick Guide to Main Model Equations and Major Assumptions of the Model

The partial differential equation that governs the quasistatic balance of linear momentum of the cell is more amenable to computational solution when it is written in weak form:

Find $u$ such that for all $w$,

$$\int \nabla^s w : \sigma[\varepsilon(u)] dV = 0, \tag{A}$$

in which $u$ is the displacement field vector, $w$ is the weighting function vector, and $\sigma[\varepsilon(u)]$ is the stress tensor, here written to emphasize its dependence on the displacement field via the strain tensor $\varepsilon(u)$. The symbol $\nabla^s$ denotes the symmetric part of the gradient operator.

**Major assumptions for equation A**

At the typical speeds of cell motility, the effect of inertia is negligible, and the "dynamic" balance of linear momentum need not be considered.

The strain tensor is defined as

$$\varepsilon(u) = \nabla^s u. \tag{B}$$

**Major assumptions for equation B**

The infinitesimal strain theory is assumed to hold, according to which nonlinear dependence of $\varepsilon$ upon $u$ can be neglected. This assumption makes for a simpler mathematical formulation and more rapid computations. The fully nonlinear theory leads to some quantitative differences in the computed stress but does not alter the results in a qualitative manner.

The stress–strain response of the actin fibers and cell membrane is governed by the constitutive equation:

$$\sigma = \lambda / tr(\varepsilon) + 2\mu\varepsilon, \tag{C}$$

in which $\lambda$ and $\mu$ are Lamé parameters defined in terms of the more familiar Young's Modulus $E$ and Poisson ratio $v$ by

$$\lambda = vE/[(1+v)(1-2v)] \quad \text{and} \quad \mu = E/2(1+v)$$

**Major assumptions for equation C**

The actin fibers and cell membrane are assumed to be elastic. This assumption implies that viscous effects associated with the kinetics of binding/unbinding of actin monomers with the cytoskeletal fibers and the lipid bilayer will not be accounted for in the stress computations. We note, however, that the purpose of the computational model in this work is to represent the kinematics of cell motility and locomotion, and not to provide a precise computation of the stress. With more appropriate viscoelastic models for the actin fibers and cell membrane, the stress computed is more physically accurate, but the fundamental conclusions reached on cell motility and locomotion do not change. The viscoelastic models also result in a more complicated mathematical formulation and slightly slower computations.

The matrix–vector version of the weak form (A) is

$$Kd = F \tag{D}$$

in which $K$ is the finite element stiffness matrix, which includes the influence of the mechanical properties, $d$ is the vector of nodal displacements, and $F$ is the external force vector. The latter includes the effect of displacement boundary conditions that model the attachment of the cell to the substrate at focal adhesions.

**Major assumptions for equation D**

Our finite element implementation is based on the plane stress model of mechanics. Plane stress is an appropriate model for the 2-dimensional shape adopted by cells on a substrate.

the MAPK pathway is effected by 4 isoforms: p38α, p38β, p38γ, and p38δ. Despite their sequence similarity and shared upstream kinases, the p38 isoforms can have unrelated, and even antagonistic, roles in development and disease (3–7).

p38γ (also known as MAPK12, ERK6, or SAPK3) is expressed predominantly in muscle tissue, where it promotes myoblast differentiation into myotubes (8–11). p38γ mRNA is overexpressed in several cancers (12, 13) and helps increase Ras-induced cancer invasion (14, 15).

Published OnlineFirst August 23, 2011; DOI:10.1158/0008-5472.CAN-11-1291



Viewing p38γ function from the developmental perspective led us to hypothesize that p38γ enables mesenchymal-like behavior in breast cancer cells by controlling their motility properties.

Using multiple mechanisms of inhibition, we reveal that p38γ is a crucial mediator of breast cancer cell motility and metastasis. Our computational model shows the central role of stress fiber orientation in p38γ-mediated cell motility. Through this *in silico* experimentation, and subsequent *in vitro* validation, we discovered a novel leading edge behavior in motile breast cancer cells. Mechanistically, p38γ elicits its effects at least in part through RhoC GTPase by affecting RhoC ubiquitination and degradation—a regulatory mechanism never before observed for RhoC. Clinically, high p38γ expression is associated with the basal-like breast cancer subtype and confers a worse prognosis. This work establishes that p38γ is a metastasis-enabling gene responsible for mediating breast cancer cell motility and metastasis, in part, by regulating cytoskeletal architecture and modulating RhoC.

## Materials and Methods

### Cell lines

Untransfected cell lines were cultured in RPMI-1640 (MDA-MB-231, BT549) or Dulbecco's Modified Eagle's Medium (DMEM; Hs578t) supplemented with 10% FBS or DMEM/Ham's F-2 (MCF-10A) supplemented with 10% horse serum. Selection media for short hairpin RNA (shRNA)-transfected MDA-MB-231 cells ("scrambled" or "shp38γ") was standard cell line media containing 1 μg/mL puromycin. MDA-MB-231 stably transfected with both shRNA and RhoC/RhoC G14V were cultured in standard cell line media containing 1 μg/mL puromycin and 350 μg/mL G418. All cell lines were grown at 37°C in a humidified 5% $CO_2$ incubator.

### Phospho-p38γ immunoprecipitation/Western blotting

Protein was extracted from 70% confluent cells with radioimmunoprecipitation assay buffer. Total protein extracts were incubated with primary antibody (anti-p38γ or anti-phospho-p38) overnight at 4°C. The following morning protein–antibody complexes were captured by incubation with protein A/G beads (Santa Cruz Biotechnology). Immunoprecipitates were run on an SDS-PAGE gel, transferred to a nitrocellulose membrane, and probed with the appropriate reciprocal antibody (anti-p38γ or anti-phospho-p38). All immunoprecipitation and Western blot data represent at least 3 independent experiments.

### *In situ* detection/quantification of protein expression

***Tumors and patients.*** resh and formalin-fixed, paraffin-embedded tissue blocks of breast cancer were obtained from the files of the Department of Pathology, University of Michigan Medical Center (Ann Arbor, MI). Institutional Review Board approval was obtained, and the diagnosis was confirmed by morphology. After pathologic review, a tissue microarray was constructed from the most representative area by the methodology of Nocito and colleagues (16). Survival data were obtained from the University of Michigan's Cancer Registry.

***Immunohistochemical staining and AQUA analysis.*** Triple immunofluorescence staining was carried out as previously described (17), and the AQUA system (HistoRx) was used for automated image acquisition and analysis. See Supplementary Materials and Methods for the detailed staining and imaging procedure.

### Orthotopic xenografts and lymphatic metastasis analysis

All mouse work was compliant with the University's standards for animal use. A total of 231 scrambled and shp38γ cells were diluted at a ratio of 1:1 with Matrigel (BD Biosciences) to a final concentration of $3 \times 10^6$ cells per mL. Athymic nude mice were anesthetized, and $1.5 \times 10^5$ cells (50 μL) were injected directly into the fourth mammary gland. Tumors were monitored weekly, and mice were euthanized once tumor volume approached 2 $cm^3$. Tumors were resected at euthanization, fixed in 10% formalin, and subsequently paraffin embedded. Hematoxylin and eosin–stained tumor sections were scored for lymphatic metastasis in a single-blind manner by Dr. J. Erby Wilkinson at the ULAM Pathology Core at the University of Michigan. Lymphatic metastasis was defined as the presence of tumor cells in the inguinal lymph node of the uninjected fourth mammary gland (the contralateral gland, relative to injection site), thus indicating the ability of tumor cells to exit the primary tumor and metastasize to distant sites through the vasculature. The number of mice presenting with lymphatic metastases was compared by the Fisher exact test. Images were captured at room temperature, using an Olympus BX-51 upright light microscope with Olympus UPlanApo ×10/0.4 numerical aperture and ×40/0.85 numerical aperture objectives and an Olympus DP-70 high-resolution digital camera with DP controller software.

### Statistical analyses

All data are representative of at least 3 independent experiments, and all error bars are mean ± SEM unless otherwise indicated. All *P* values were calculated by the Student 2-tailed *t* test unless otherwise noted. Expression levels of p38γ and RhoC in tissue microarray samples were compared using Spearman rank correlation coefficient. Associations between p38γ and breast cancer subtype and the prevalence of lymphatic metastasis between scrambled and shp38γ cells were determined by the Fisher exact test. The relationship between p38γ expression and patient survival was calculated by Kaplan–Meier analysis, with surviving patients censored. The log-rank test statistic was used for significance.

## Results

### p38γ phosphorylation is elevated in an aggressive breast cancer cell line

p38 is activated by dual phosphorylation of the threonine and tyrosine residues of the conserved TGY motif (3, 18). To assess p38γ functional relevance in aggressive breast cancer, we assayed phospho-p38γ levels in a representative and widely used aggressive breast cancer cell line, MDA-MB-231 ("231

Published OnlineFirst August 23, 2011; DOI:10.1158/0008-5472.CAN-11-1291



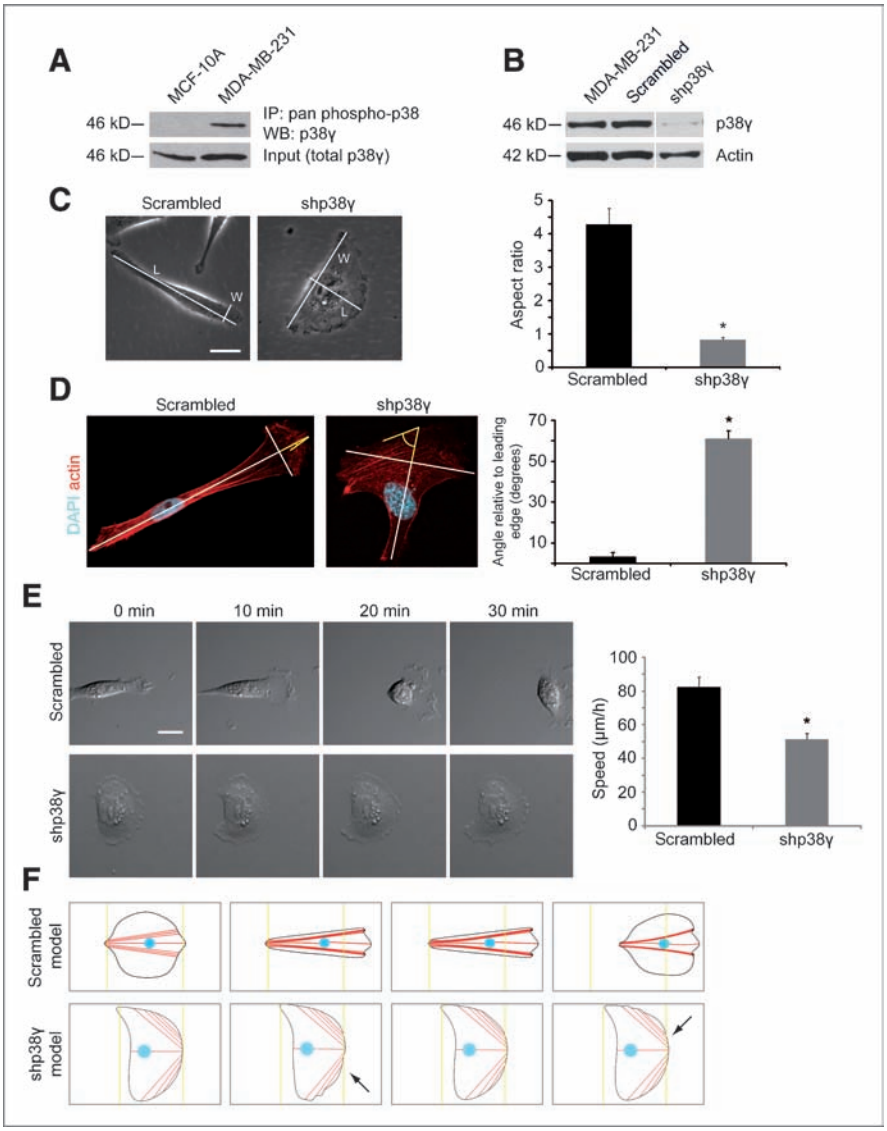


Figure 1. p38γ affects MDA-MB-231 cell motility and may do so by shaping the actin cytoskeleton. A, phospho-p38γ levels are elevated in the MDA-MB-231 breast cancer cell line compared with nontumorigenic MCF-10A mammary epithelial cells. B, shRNA knockdown of p38γ in MDA-MB-231 cells. C, left, cell shapes of scrambled and shp38γ cells. Right, quantification of cell shape difference by aspect ratio measurement (*L*/*W*: length/width; *, $P = 7.82 \times 10^{-7}$, $n = 22$ cells for scrambled, $n = 27$ cells for shp38γ; scale bar, 25 μm). D, actin fiber orientation differs between scrambled and shp38γ cells. (*, $P = 1.96 \times 10^{-7}$, $n = 16$ for scrambled, $n = 22$ for shp38γ; scale bar, 20 μm). E, left, representative images from time-lapse movies (Supplementary Movies S1 and S2) of scrambled and shp38γ cells, showing the characteristic mesenchymal-like motility of scrambled cells (top) and the disjoint crawling motion of shp38γ cells (bottom; scale bar, 10 μm). Right, shp38γ cells are significantly slower than scrambled cells (*, $P = 3.34 \times 10^{-5}$, $n = 30$ cells per cell line). F, preliminary computational models of scrambled and shp38γ cells qualitatively represent the locomotion of each cell type (see text for details). Arrows point to out-of-phase lamellipodial oscillations. The actin fibers are in red and the nucleus is in blue. DAPI, 4′,6-diamidino-2-phenylindole; IP, immunoprecipitation; WB, Western blot.

cells"). Compared with the nontumorigenic mammary epithelial cell line MCF-10A, MDA-MB-231 cells have increased levels of phosphorylated p38γ, despite similar levels of total p38γ (Fig. 1A).

To investigate the role of p38γ on the metastatic features of MDA-MB-231 cells, we used shRNA to stably knock down p38γ expression (Fig. 1B). Importantly, the shRNA did not affect expression of the other 3 p38 isoforms (Supplementary Fig. S1A). Because there is no p38γ-specific pharmacologic inhibitor, we overexpressed dominant-negative p38γ (DNp38γ; ref. 19) in MDA-MB-231 cells as an additional inhibition method (See Supplementary Materials and Methods and Supplementary Fig. S2).

### p38γ knockdown alters cell shape and cytoskeletal architecture

Immediately apparent in the p38γ knockdown cells (shp38γ cells) was an altered cell morphology compared with scrambled control cells (scrambled cells). Although scrambled cells exhibited the elongated morphology characteristic of MDA-MB-231 cells and mesenchymal cells in general, shp38γ cells adopted a more rounded shape (Fig. 1C), as did DNp38γ cells (Supplementary Fig. S2C). This change was quantified by the aspect ratio of cells (see Supplementary Materials and Methods). As depicted in Fig. 1C (right), shp38γ cells are significantly less elongated than scrambled cells.

We further asked whether the actin cytoskeleton was modified in shp38γ cells. Immunofluorescent confocal microscopy revealed that shp38γ cells have a strikingly disorganized actin cytoskeleton (Fig. 1D), as do DNp38γ cells (Supplementary Fig. S2E). Scrambled cells exhibit mesenchymal-like polarization with cell-length stress fibers oriented at 3.42 ± 1.89 degrees (mean ± SD) on either side of the normal to the leading edge (Fig. 1D). shp38γ cells retain thick actin bundles resembling stress fibers but primarily confined to the leading edge and with a bimodal orientation distribution at 61.08 ± 3.94 degrees (mean ± SD; Fig. 1D). This cluster of actin bundles forms the lamellipodia-like structure present in

Published OnlineFirst August 23, 2011; DOI:10.1158/0008-5472.CAN-11-1291



shp38γ cells (Fig. 1C and D) but shows little similarity to classic lamellipodial cytoskeletal architecture, which normally consists of thin, branched actin filaments forming a protrusive meshwork (20).

**p38γ knockdown dramatically alters cell motility and affects other *in vitro* metastasis-associated properties of MDA-MB-231 cells**

Elongated cell shape is one factor that delineates both the mode of motility used by a cell and metastatic from nonmetastatic cancer cells *in vitro* (21, 22). To determine whether the rounded shape and modified cytoskeletal architecture of shp38γ cells indicated a change in metastatic properties, we first analyzed cell motility—specifically unstimulated random walk—by time-lapse microscopy.

p38γ knockdown profoundly affected the quality of cell motility (Fig. 1E, left) and their speed (Fig. 1E, right). Scrambled control cells had a mesenchymal-like motility, consistent with their appearance and cytoskeletal structure, using long pseudopodial projections to "pull" themselves along in alternating cycles of protrusion and contraction (Fig. 1E, top left, and Supplementary Movie S1). shp38γ cells, however, remained unpolarized and were unable to form long pseudopodia (Fig. 1E, bottom left, and Supplementary Movie S2). The cells moved inefficiently using broad lamellipodia-like structures and exhibited detachment anomalies at the rear of the cell. Quantitatively, p38γ knockdown significantly reduced cell speed (Fig. 1E, right).

We also investigated p38γ function in cancer cell invasion and aggressive 3-dimensional growth and found that p38γ knockdown significantly impaired both properties (Supplementary Fig. S1B and S1C). These data show that p38γ knockdown affects the *in vitro* metastasis-related properties of aggressive breast cancer cells and specifically inhibits efficient mesenchymal-like motion in a qualitative and quantitative manner.

**Computational modeling reveals that p38γ-induced changes in cytoskeletal architecture influence cell motility**

We observed that p38γ knockdown had functional (impaired motility and other metastasis-related properties) and structural (actin cytoskeleton and cell shape) effects on MDA-MB-231 cells. However, there remained the question of whether the change in actin cytoskeletal structure is sufficient to explain the observed impairment of motility. Because it remains inaccessible to experiments, this central question was addressed by computational modeling.

Our computational models use the finite element method to solve the partial differential equations governing the mechanics of cell motility (see Supplementary Materials and Methods for details). We hypothesized that the strikingly different cytoskeletal architectures—polarized stress fibers in scrambled versus bimodal bundles of fibers in shp38γ cells—underlie the observed differences in motility.

To test this hypothesis, we first created a computational model of scrambled cell motility. Using the typical dimensions of scrambled cells (Supplementary Table S2; Fig. 1C), their observed cytoskeletal morphology of ±3.42 degrees (Fig. 1D), and the mechanical properties of actin fibers and cell membranes of mammalian cells (Supplementary Table S1), we varied the rates of actin filament protrusion and retraction as model inputs to successfully recreate the observed locomotion of live scrambled cells (Fig. 1F, top, and Supplementary Movie S3).

To determine whether actin cytoskeletal architecture delineates the motility of the 2 MDA-MB-231 phenotypes, we next created a computational model of shp38γ cells, using the dimensions reported in Supplementary Table S2 and Fig. 1C, the cytoskeletal morphology of actin bundles at ±61.08 degrees (Fig. 1D and Supplementary Fig. S3), and the same mechanical properties of actin fibers and cell membrane as for the scrambled cells (Supplementary Table S1). We further conjectured, and computationally showed, that the observed oscillations in motion of shp38γ cells that are evident in Supplementary Movie S2 were only possible if the 2 families of actin bundles at ±61.08 degrees alternate (are out of phase) in their protrusion/retraction (data not shown). When incorporated, these alternating dynamics, albeit not precisely timed, produced a disjoint crawling motion with oscillations of the cell body of the computational shp38γ cell. This motility was remarkably similar to our live shp38γ cell motility (Fig. 1E, bottom, and Supplementary Movie S3), suggesting that actin cytoskeletal architecture is important for defining shp38γ cell motility. However, further experiments were necessary to separate the influence of actin fiber orientation from actin protrusion/retraction dynamics.

**Live scrambled and shp38γ cells have oscillating leading edge protrusions related to modified cytoskeletal architecture**

The computational shp38γ cell motility thus revealed the possibility of a previously unobserved aspect of cellular dynamics, namely, waves of oscillating left- and right-of-center protrusion at the leading edge of a migrating cell. To test this model prediction, we studied in detail the dynamic behavior of the leading edge of scrambled and shp38γ cells stably transfected with red fluorescent protein (RFP)-actin.

Using time-lapse microscopy and image edge detection techniques (Supplementary Materials and Methods), we observed remarkable differences in leading edge protrusion between scrambled and shp38γ cells (Fig. 2A and C). At first observation, scrambled cells appeared to protrude in one continuous motion whereas shp38γ cells had alternating left- and right-of-center protrusions, corresponding to the 2 families of actin bundles at ±61.08 degrees (Fig. 2A). Upon closer analysis, leading edge protrusion in *both* cell lines actually manifested alternations between left- and right-of-center leading edge regions (Fig. 2B and C). (In the case of scrambled cells, these regions correspond to the stress fibers at ±3.42 degrees.) However, the cell lines were distinguished by the time half-period between left and right protrusions being much longer (4.83 ± 1.09 minutes) in shp38γ cells than in scrambled cells (1.75 ± 0.14 minutes; Fig. 2D). This periodicity is evident in the time-lapse movies as the disjoint crawling motion of shp38γ cells (Supplementary Movie S2),

Published OnlineFirst August 23, 2011; DOI:10.1158/0008-5472.CAN-11-1291



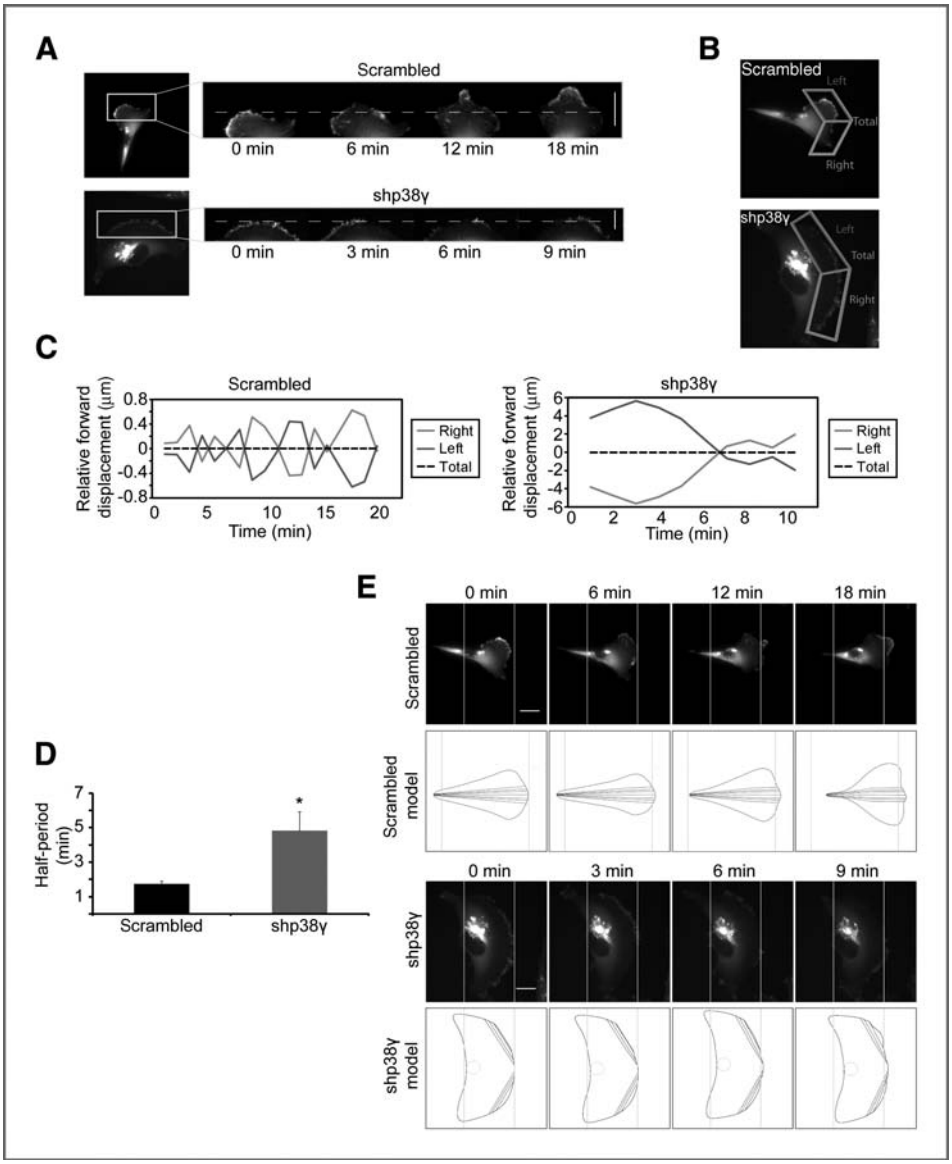


Figure 2. The leading edge protrusion dynamics predicted by the computational shp38γ model occur in live cells and these behaviors differ between scrambled and shp38γ cells. A, kymographs of leading edge protrusion in scrambled and shp38γ cells. B, detail showing the "left" and "right" sides of the leading edges of scrambled and shp38γ cells. C and D, dynamics of left and right sides of cell leading edges. Leading edge protrusions from the highlighted regions in (B) are represented graphically (C). The reference is set such that mean forward displacement equals zero; thus, forward displacement greater than the mean of left and right appears positive and forward displacement less than the mean appears negative. D, the half-period in (C; average time between left-right intersections) is significantly greater for shp38γ cells than scrambled cells (*, $P = 0.0072$, $n = 3$ for each cell line). E, time-lapse images of RFP-actin–transfected scrambled (top) and shp38γ (bottom) cells, with finite element computations for each cell type shown below the corresponding live cell images (from Supplementary Movie S4; scale bar, 20 μm). Together with Supplementary Fig. S4, this validates our computational mechanical model of whole-cell locomotion using subcellular motility data.

contrasting with the coordinated protrusion/retraction cycle of scrambled cells (Supplementary Movie S1). Also note the larger amplitudes of leading edge protrusions in shp38γ cells (Fig. 2C).

These live cell results confirmed the computational model predictions. We repeated our computational cell motility studies with the mean left/right leading edge protrusion amplitudes and time periods, and trailing edge retraction rates (Supplementary Fig. S4A), which we measured via time-lapse microscopy, now used as targets to be met by controlling the actin fiber extension/contraction rates in the model (Supplementary Materials and Methods). Incorporating these experimentally measured dynamics further refined our computational models, showed good agreement between the live and computational cells, and importantly did not fundamentally alter the refined computational cell model results from the initial ones in a qualitative sense (compare Figs. 1F and 2E; Supplementary Movie S4). Through a series of additional control computational simulations (Supplementary Fig. S4 and Supplementary Results), we determined that, other parameters remaining the same, modifications in cytoskeletal architecture alone are sufficient to influence cell motility in the manner observed experimentally—from creating effective locomotion in live scrambled cells to ineffective locomotion of shp38γ cells.

### Expression of the cytoskeletal remodeler and metastasis-promoting gene *RhoC* is decreased in shp38γ cells

Rho-family GTPases (Rac, Rho, and cdc42) are the classic regulators of actin cytoskeletal dynamics driving cell motility (23). On the basis of the actin cytoskeletal changes and motility defects we observed, we hypothesized that p38γ

Published OnlineFirst August 23, 2011; DOI:10.1158/0008-5472.CAN-11-1291



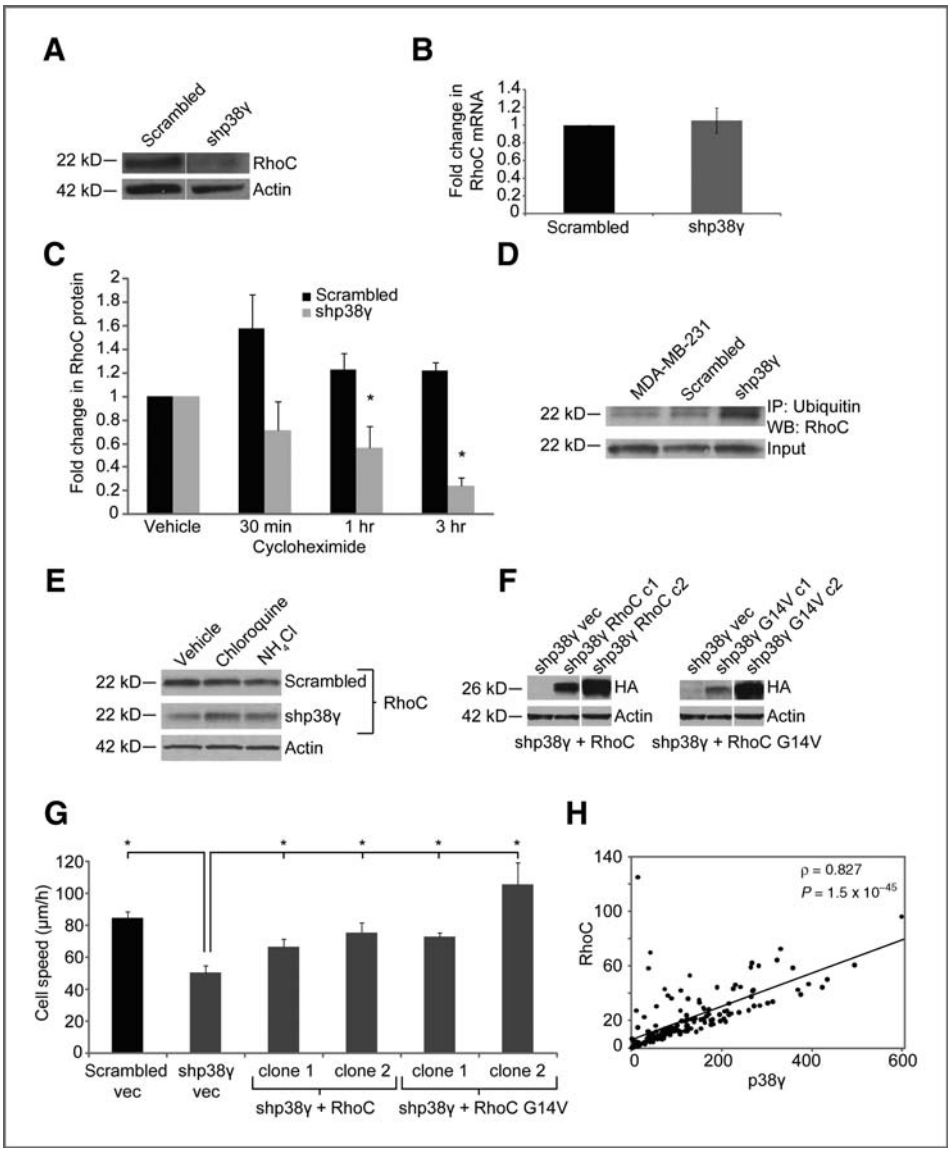


Figure 3. p38γ affects RhoC expression by mediating RhoC ubiquitination and lysosomal degradation. Expression of RhoC GTPase protein (A) but not mRNA (B) is significantly reduced by p38γ knockdown. C, cycloheximide treatment reveals that RhoC protein is less stable in shp38γ cells. *, $P < 0.05$. D, RhoC ubiquitination is increased in shp38γ cells. E, RhoC is degraded by the lysosome, as treatment with lysosome inhibitors leads to an increase in RhoC protein in shp38γ cells. F, shp38γ cells were stably transfected with either hemagglutinin (HA)-tagged RhoC (left) or a constitutively active form of RhoC, RhoC G14V (right). Two clones—1 high expressing and 1 low expressing—were selected for each construct. G, reexpressing RhoC in shp38γ cells significantly increases shp38γ cell speed to levels comparable with scrambled cells (*, $P < 0.05$). H, expression of p38γ and RhoC is strongly positively correlated in clinical breast cancer samples ($n = 177$, $\rho = 0.827$, $P = 1.5 \times 10^{-45}$). Vec, vector; WB, Western blot.

knockdown affected the members of the Rho GTPase family. Interestingly, we found that RhoC GTPase protein levels were downregulated in both shp38γ and DNp38γ cells (Fig. 3A and Supplementary Fig. S2F), with no change in the close homolog RhoA (data not shown). Surprisingly, RhoC mRNA levels were unaffected by p38γ knockdown (Fig. 3B), suggesting that p38γ influences RhoC expression at the translational or posttranslational level.

### p38γ knockdown leads to increased RhoC ubiquitination and degradation

To determine whether p38γ affects RhoC expression at the translational or posttranslational level, we treated scrambled and shp38γ cells with the translation inhibitor cycloheximide and observed the effect on protein expression. Cycloheximide treatment caused RhoC protein levels to rapidly decrease in shp38γ cells, with no corresponding decrease in scrambled cells (Fig. 3C), indicating that RhoC protein is less stable in shp38γ cells.

Upon observing this change in stability, we asked whether RhoC was ubiquitinated in shp38γ cells—a common marker of proteins slated for degradation. Upon assaying RhoC ubiquitination, we found that levels of ubiquitinated RhoC were increased in shp38γ compared with scrambled cells (Fig. 3D).

To elucidate the RhoC degradation mechanism, we treated cells with either proteasome inhibitors (MG132 or lactacystin) or lysosome inhibitors (ammonium chloride or chloroquine) and observed the effect on RhoC protein levels. Lysosome inhibition caused an increase in RhoC protein (Fig. 3E), whereas proteasome inhibitors had no effect on RhoC expression (Supplementary Fig. S1D), indicating that ubiquitinated RhoC is degraded by the lysosome. Taken together, these data support the conclusion that p38γ affects RhoC expression by

Published OnlineFirst August 23, 2011; DOI:10.1158/0008-5472.CAN-11-1291



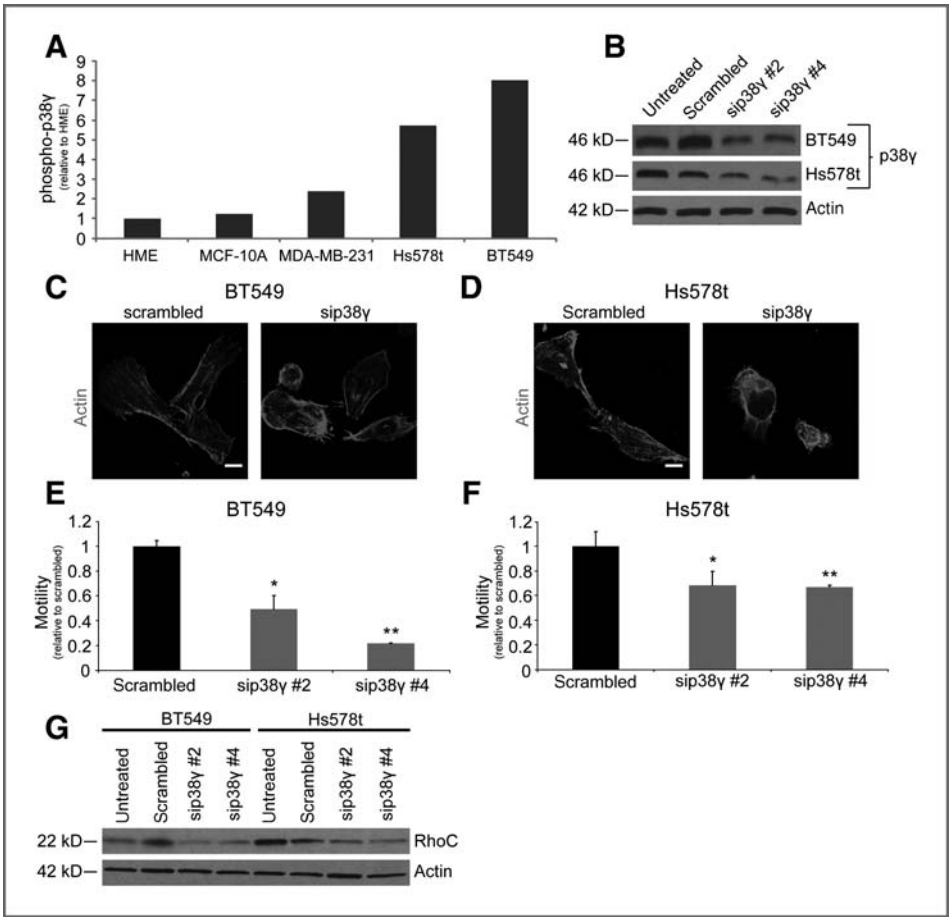


Figure 4. p38γ functions similarly in 2 additional aggressive breast cancer cell lines. A, levels of phospho-p38γ are elevated in the MDA-MB-231, Hs578t, and BT549 breast cancer cell lines compared with both HME and MCF-10A nontumorigenic mammary epithelial cells. Graph shows (immunoprecipitation) IP/input (phospho-p38γ/total p38γ) quantification of a representative Western blot. B, transient sip38γ in BT549 and Hs578t cells. The siRNA did not affect the other p38 isoforms (data not shown). C and D, the actin cytoskeleton and cell shape of sip38γ BT549 (C) and Hs578t (D) cells are altered in a manner similar to 231 shp38γ cells (scale bar, 25 μm). E and F, p38γ knockdown significantly reduces cell motility as measured by a bead motility assay in BT549 (E) and Hs578t (F) cells (for 2 BT549 siRNAs: *, $P = 0.0428$; **, $P = 1.64 \times 10^{-5}$; for 2 Hs578t siRNAs: *, $P = 0.0001$; **, $P = 0.0012$). G, RhoC expression is reduced in siRNA-transfected BT549 and Hs578t cells.

mediating RhoC protein stability through regulation of RhoC ubiquitination and lysosomal degradation.

### Rescuing RhoC expression restores motility to shp38γ cells

On the basis of the established roles of RhoC in cell motility and metastasis (24, 25), we hypothesized that decreased RhoC expression in shp38γ cells directly contributes to the impaired motility of shp38γ cells. To test this hypothesis, we stably transfected either RhoC or a constitutively active variant (RhoC G14V) into shp38γ cells and observed the effect on cell motility (Fig. 3F).

Live cell microscopy revealed that reexpressing RhoC significantly increased motility of the shp38γ cells to levels comparable with scrambled control cells (Fig. 3G). Interestingly, the cell speed increase seemed to have a near-linear relationship with RhoC expression/activity. Combined with our previous observations, these data establish a novel mechanistic link whereby p38γ directs cell motility through stabilization of RhoC protein.

### p38γ and RhoC expression is strongly positively correlated in human breast cancer tissues

We next asked whether the p38γ–RhoC relationship persists in human breast cancer tissues. To address this question we assayed expression of p38γ and RhoC using AQUA of immunofluorescence signals for each marker in cytokeratin-positive cells from a breast cancer tissue microarray. Analysis of 177 breast cancer specimens revealed a strong positive correlation between p38γ and RhoC expression (Fig. 3H). Taken together with our *in vitro* results, these data strongly support a p38γ–RhoC relationship in breast cancer, one that likely involves p38γ regulation of RhoC expression.

### p38γ affects the metastatic properties of other aggressive breast cancer cell lines

Because p38γ specifically alters the actomyosin contractile motility of MDA-MB-231 cells by affecting RhoC expression, we asked whether it plays a similar role in other mesenchymal-like breast cancer cell lines. To address this question, we used 2 additional widely studied breast cancer cell lines—Hs578t and BT549—both of which have increased levels of phosphorylated p38γ compared with both MCF-10A and HME nontumorigenic mammary epithelial cells (Fig. 4A). We transiently knocked down p38γ expression in these 2 cell lines with siRNA (Fig. 4B) and observed the effects on the actin cytoskeleton and cell motility.

siRNA knockdown of p38γ (sip38γ) dramatically affected the actin cytoskeletal architecture and cell shape of both cell lines in a manner consistent with 231 shp38γ cells (Fig. 4C and

Published OnlineFirst August 23, 2011; DOI:10.1158/0008-5472.CAN-11-1291



D): sip38γ cells moved significantly less than scrambled cells (Fig. 4E and F). p38γ knockdown in these cell lines also reduced RhoC expression (Fig. 4G). Taken together, these results support our conclusion that p38γ plays a crucial role in promoting motility of aggressive breast cancer cells by modulating RhoC expression.

### p38γ is associated with the basal-like breast cancer subtype

Having discovered that p38γ is associated with mesenchymal-like cell motility and is overactivated in 3 basal-like breast cancer cell lines, we hypothesized that p38γ is associated with the basal-like breast cancer subtype. To test this hypothesis, we assayed p38γ expression in samples of 43 patients with breast cancer who were previously analyzed for molecular subtype by PAM50 (26). We divided the cohort into high (top 25%) and low (bottom 75%) p38γ-expressing tumors and examined the association between p38γ expression level and molecular subtype. We found that the basal-like subtype is significantly enriched in the high p38γ-expressing tumors ($P = 0.018$, Fig. 5A) whereas none of the other subtypes examined showed significant association with p38γ expression (data not shown). Taken together with our *in vitro* data, these clinical data strongly support an association between high p38γ expression and the basal-like breast cancer subtype.

### p38γ is necessary for breast cancer metastasis *in vivo* and is clinically associated with lower overall patient survival

On the basis of our *in vitro* observations, we hypothesized that p38γ knockdown reduces the metastatic potential of MDA-MB-231 breast cancer cells *in vivo*. To test this hypothesis, we orthotopically xenografted athymic nude mice with 231 scrambled and shp38γ cells and allowed tumors to grow for 14 weeks, at which point we resected the tumors and analyzed the contralateral respective lymph node for signs of metastasis (see Supplementary Materials and Methods). Two thirds of mice injected with scrambled cells presented with

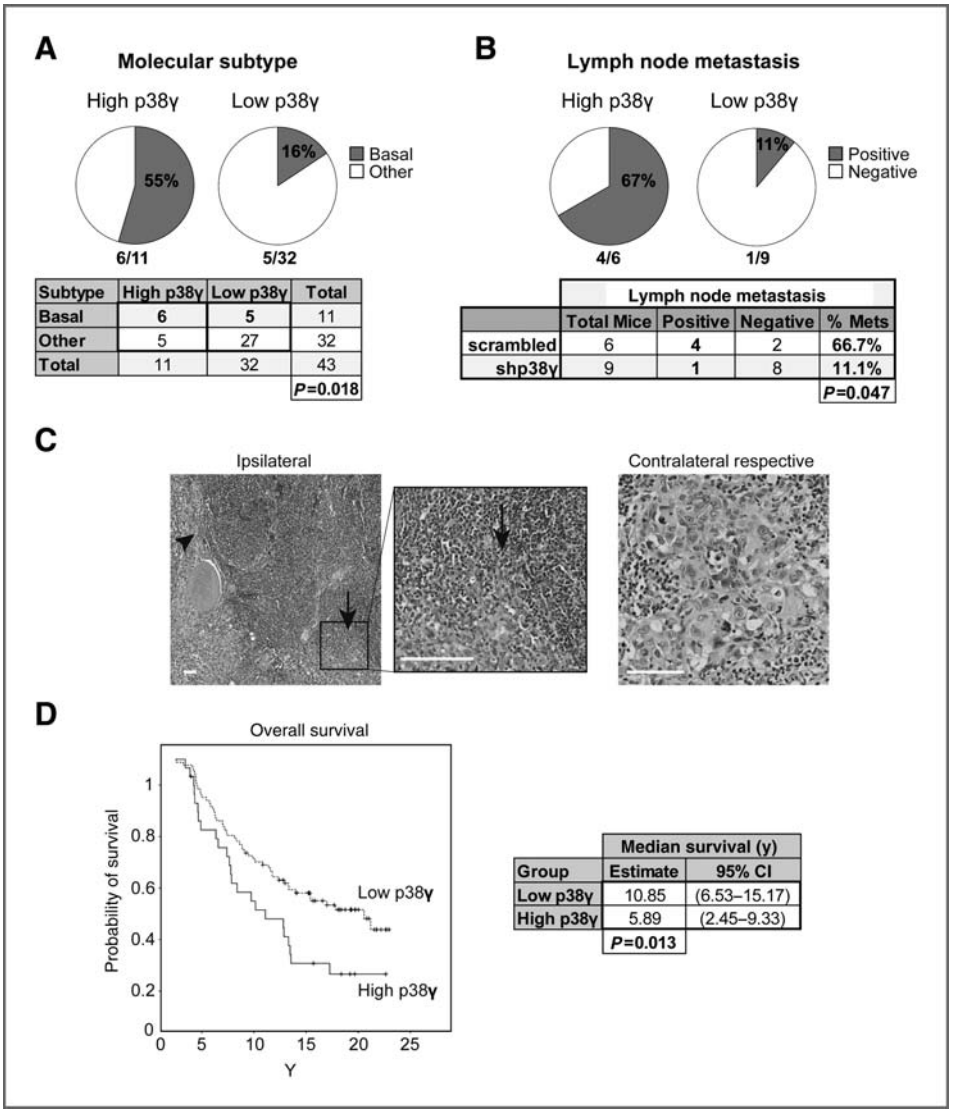


| Subtype | High p38γ | Low p38γ | Total |
|---|---|---|---|
| Basal | 6 | 5 | 11 |
| Other | 5 | 27 | 32 |
| Total | 11 | 32 | 43 |
| | | | $P$=0.018 |

| | Lymph node metastasis | | | |
|---|---|---|---|---|
| | Total Mice | Positive | Negative | % Mets |
| scrambled | 6 | 4 | 2 | 66.7% |
| shp38γ | 9 | 1 | 8 | 11.1% |
| | | | | $P$=0.047 |

| | Median survival (y) | |
|---|---|---|
| Group | Estimate | 95% CI |
| Low p38γ | 10.85 | (6.53–15.17) |
| High p38γ | 5.89 | (2.45–9.33) |
| | $P$=0.013 | |

Figure 5. p38γ is associated with the basal-like breast cancer subtype and impacts metastasis and patient survival. A, the basal-like breast cancer subtype is enriched in high (top 25%) compared with low (bottom 75%) p38γ-expressing patients ($P = 0.018$). B, quantification of lymph node metastasis of orthotopically xenografted 231 scrambled and shp38γ cells. Scrambled cells had a significantly higher incidence of metastasis into the contralateral mammary lymph nodes ($P = 0.047$), as measured by the Fisher exact test. C, representative images of 231 scrambled cells invading the ipsilateral lymph node (left) and a metastatic cluster in the contralateral respective mammary gland (right). The intact lymph node capsule is indicated by the arrowhead, whereas invading scrambled cells are marked by the arrow and magnified in the inset (all scale bars, 100 μm). D, high p38γ expression is associated with lower overall survival of patients with breast cancer, as determined by Kaplan–Meier analysis ($P = 0.013$). CI, confidence interval.

Published OnlineFirst August 23, 2011; DOI:10.1158/0008-5472.CAN-11-1291



lymphatic invasion and metastasis compared with 1 of 9 shp38γ-injected mice (Fig. 5B and C). These *in vivo* data, combined with the extensive body of *in vitro* data presented here, strongly suggest that p38γ is necessary for metastasis and that it exerts its effects, at least in part, by promoting cell motility through regulation of RhoC.

As a final determination of the clinical relevance of p38γ expression, we assayed p38γ levels in a cohort of 118 breast cancer cases containing patient survival data. Using the same high/low cutoff values as the molecular subtype analysis, we found a significant association between high p38γ expression and lower overall patient survival ($P = 0.013$, Fig. 5D). These clinical data support our *in vitro* and *in vivo* findings that p38γ is an important mediator of breast cancer cell aggressiveness, establishing that p38γ expression has important implications for outcome of patients with breast cancer.

## Discussion

Because the breast is a nonvital organ, primary tumor burden is very rarely the direct cause of cancer-specific mortality. Instead, metastasis of cells from the primary tumor to vital organs results in patient death. Here, we show that *p38γ* is a novel metastasis-associated gene, which acts in part by affecting cytoskeletal orientation, cell motility, and RhoC.

The importance of the p38 MAPK pathway in cancer has been appreciated (6, 27), but diverse, and sometimes contradictory, roles have been described for p38 in cancer (13). In agreement with other recent findings (15, 28), we show that at least some of the discrepancy in p38 function may be attributed to the distinct contributions of p38 isoforms. The p38 MAPK pathway is ubiquitously used in stress response. It logically follows that metastasizing cancer cells, which encounter an ever-changing milieu of cellular stresses, may gain survival advantages under stressed conditions upon modulation of the appropriate p38 MAPK isoforms; thus, dissecting the contributions of each p38 isoform would allow more precise targeting of specific subsets of cancer. p38γ is an especially promising drug target, as, in addition to the data presented here, it is a kinase, has restricted tissue expression (8, 10, 11), and lacks a phenotype when knocked out in mice (29)—possibly indicating that its inhibition may offer a differential detrimental effect on tumor versus normal cells.

Using a computational cell model in combination with live cell microscopy studies, we showed that p38γ promotes breast cancer cell motility at least in part by mediating actin cytoskeletal remodeling to create proper stress fiber orientation. Using the computational cell models, we first noted that whereas the observed whole-cell locomotion could be produced by simultaneous action of all stress fibers in scrambled cells, the experimentally observed ineffective locomotion of shp38γ cells was only possible if the action alternated between the 2 families of actin bundles seen in this cell phenotype—a result that would prove difficult to show by cell biologic techniques alone.

The computational model predicted, and subsequent biologic experiments verified, the presence of left-right leading edge protrusion oscillations in both scrambled and shp38γ cells. We note that other groups have identified oscillations in components of the leading edge (30, 31); however, these oscillations all involved forward–backward (protrusion/retraction) movement of the leading edge as a whole. To the best of our knowledge, the data presented here are thus the first evidence of left-right oscillations in the leading edge. Interestingly, the principal difference between the 2 cell types studied here (scrambled and shp38γ) lies in the periodicity of these oscillations. Through detailed *in silico* experimentation (Fig. 2, Supplementary Fig. S4), we determined that leading edge protrusion oscillation periodicity is influenced by and inseparable from cytoskeletal architecture. This inseparability sharpens the question of exactly how leading edge actin dynamics are linked to cell shape and cytoskeletal morphology. Although this is a subject for future investigation, we do speculate on the chain of events: p38γ knockdown results in cytoskeletal architecture changes, which lead to alteration of cell shape, compensatory changes in leading edge protrusion periodicity, and ultimately modified whole-cell motility.

Oscillation of other components of cell motility, such as cell shape (32) and trailing edge retraction (33), has been shown to be essential for productive cell motion in *Dictyostelium discoideum* (32) and fish keratocytes (33). We expect further investigations to uncover links between these processes and leading edge protrusion oscillations.

p38γ bears analogies with other mediators of normal mesenchymal differentiation such as twist and snail, which have also been shown to be important promoters of cancer progression (34, 35): p38γ functions in muscle cell differentiation and thus it is consistent that it functions in mesenchymal-like breast cancer cells. Interestingly, p38γ seems to exert its effects independently of classical cell differentiation markers, as p38γ knockdown does not alter expression of epithelial-to-mesenchymal transition markers such as vimentin or E-cadherin (data not shown) despite significantly reverting the mesenchymal-like phenotype of aggressive breast cancer cells. Although many other genes have been shown to drive metastatic transition (36), based on the data presented here, we propose that p38γ serves as a crucial regulator of the major cytoskeletal changes necessary for the switch to rapid, mesenchymal-like cell motility—independent of differentiation status—at least in part by modulating RhoC.

RhoC is involved in stress fiber formation and actomyosin contraction (37, 38)—both of which are perturbed by p38γ knockdown—and has previously been linked to the p38 MAPK pathway (39). RhoC also drives metastasis in several types of cancer, including breast cancer (37, 40–42), and plays a larger role in stress fiber formation and contraction than RhoA (43); thus, we postulated that changes in RhoC expression influence the shp38γ phenotype. Supporting this hypothesis, we found that reexpressing RhoC alone was sufficient to restore motility to shp38γ cells—a surprising feat, given the multitude of proteins involved in cell motility (44, 45), which highlights the importance of RhoC in p38γ-mediated cell motility. Further supporting the p38γ–RhoC link is our finding that expression of the 2 proteins is concurrently altered in

clinical breast cancer specimens (Fig. 5A), suggesting that the p38γ–RhoC axis may be functionally significant—and a potentially druggable target—in the clinic.

We discovered that p38γ regulates RhoC expression by preventing RhoC ubiquitination and subsequent lysosomal degradation. Although other p38 isoforms have been linked to protein ubiquitination (46, 47), ours is the first evidence of p38γ contributing to this process. Ubiquitination and protein degradation have recently emerged as important mechanisms for regulating Rho GTPase expression (48); however, this is the first demonstration of modulating RhoC ubiquitination as a relatively fast mechanism to regulate RhoC action within a time domain relevant to cell motion. Further research into the specific proteins and mechanisms regulating ubiquitination of RhoC and other Rho GTPases should have significant impact on our understanding of how cell motility and metastasis are regulated.

## Disclosure of Potential Conflicts of Interest

No potential conflicts of interest were disclosed.

Sofia D. Merajver, one of the Senior Editors of *Cancer Research*, is a coauthor of this article. In keeping with the AACR's Editorial Policy, the paper was peer reviewed and a member of the AACR's Publications Committee rendered the decision concerning acceptability.

## Acknowledgments

The authors thank the University of Michigan Microscopy and Image Analysis laboratory for excellent technical support with all microscopy work, Dr. J. Erby Wilkinson and the ULAM Pathology Core for tissue processing and pathologic analysis, and Dr. Dafydd Thomas and the UMCCC Tissue Core for carrying out the AQUA staining and image acquisition.

## Grant Support

This work was supported by the Department of Defense Breast Cancer Research Program through a Predoctoral Traineeship award (BC083262; to D.T. Rosenthal) and a Multidisciplinary Postdoctoral award (A.C. Ventura), an NIH Cellular and Molecular Biology Training grant (T32-GM07315; D.T. Rosenthal), the Burroughs Wellcome Fund (S.D. Merajver), the Breast Cancer Research Foundation (S.D. Merajver), and a Department of Energy PECASE award (K. Garikipati). A.C. Ventura is a member of the Carrera del Investigador Científico (CONICET).

The costs of publication of this article were defrayed in part by the payment of page charges. This article must therefore be hereby marked *advertisement* in accordance with 18 U.S.C. Section 1734 solely to indicate this fact.

Received April 14, 2011; revised July 22, 2011; accepted August 5, 2011; published OnlineFirst August 23, 2011.

## References

1. Burstein HJ, Polyak K, Wong JS, Lester SC, Kaelin CM. Ductal carcinoma *in situ* of the breast. N Engl J Med 2004;350:1430–41.
2. Chang L, Karin M. Mammalian MAP kinase signalling cascades. Nature 2001;410:37–40.
3. Cuenda A, Rousseau S. p38 MAP-kinases pathway regulation, function and role in human diseases. Biochim Biophys Acta 2007;1773:1358–75.
4. Wang Y, Huang S, Sah VP, Ross J Jr, Brown JH, Han J, et al. Cardiac muscle cell hypertrophy and apoptosis induced by distinct members of the p38 mitogen-activated protein kinase family. J Biol Chem 1998;273:2161–8.
5. Platanias LC. Map kinase signaling pathways and hematologic malignancies. Blood 2003;101:4667–79.
6. Wagner EF, Nebreda AR. Signal integration by JNK and p38 MAPK pathways in cancer development. Nat Rev Cancer 2009;9:537–49.
7. Qi X, Pohl NM, Loesch M, Hou S, Li R, Qin JZ, et al. p38alpha antagonizes p38gamma activity through c-Jun-dependent ubiquitin-proteasome pathways in regulating Ras transformation and stress response. J Biol Chem 2007;282:31398–408.
8. Tortorella LL, Lin CB, Pilch PF. ERK6 is expressed in a developmentally regulated manner in rodent skeletal muscle. Biochem Biophys Res Commun 2003;306:163–8.
9. Cuenda A, Cohen P. Stress-activated protein kinase-2/p38 and a rapamycin-sensitive pathway are required for C2C12 myogenesis. J Biol Chem 1999;274:4341–6.
10. Wang XS, Diener K, Manthey CL, Wang S, Rosenzweig B, Bray J, et al. Molecular cloning and characterization of a novel p38 mitogen-activated protein kinase. J Biol Chem 1997;272:23668–74.
11. Li Z, Jiang Y, Ulevitch RJ, Han J. The primary structure of p38 gamma: a new member of p38 group of MAP kinases. Biochem Biophys Res Commun 1996;228:334–40.
12. Tang J, Qi X, Mercola D, Han J, Chen G. Essential role of p38gamma in K-Ras transformation independent of phosphorylation. J Biol Chem 2005;280:23910–7.
13. Loesch M, Chen G. The p38 MAPK stress pathway as a tumor suppressor or more? Front Biosci 2008;13:3581–93.
14. Qi X, Tang J, Loesch M, Pohl N, Alkan S, Chen G. p38gamma mitogen-activated protein kinase integrates signaling crosstalk between Ras and estrogen receptor to increase breast cancer invasion. Cancer Res 2006;66:7540–7.
15. Loesch M, Zhi HY, Hou SW, Qi XM, Li RS, Basir Z, et al. p38{gamma} MAPK cooperates with c-Jun in trans-activating matrix metalloproteinase 9. J Biol Chem 2010;285:15149–58.
16. Nocito A, Kononen J, Kallioniemi OP, Sauter G. Tissue microarrays (TMAs) for high-throughput molecular pathology research. Int J Cancer 2001;94:1–5.
17. McCabe A, Dolled-Filhart M, Camp RL, Rimm DL. Automated quantitative analysis (AQUA) of in situ protein expression, antibody concentration, and prognosis. J Natl Cancer Inst 2005;97:1808–15.
18. Cohen P. The search for physiological substrates of MAP and SAP kinases in mammalian cells. Trends Cell Biol 1997;7:353–61.
19. Enslen H, Raingeaud J, Davis RJ. Selective activation of p38 mitogen-activated protein (MAP) kinase isoforms by the MAP kinase kinases MKK3 and MKK6. J Biol Chem 1998;273:1741–8.
20. Ladwein M, Rottner K. On the Rho'd: the regulation of membrane protrusions by Rho-GTPases. FEBS Lett 2008;582:2066–74.
21. Rajah TT, Abidi SM, Rambo DJ, Dmytryk JJ, Pento JT. The motile behavior of human breast cancer cells characterized by time-lapse videomicroscopy. In Vitro Cell Dev Biol Anim 1998;34:626–8.
22. Partin AW, Schoeniger JS, Mohler JL, Coffey DS. Fourier analysis of cell motility: correlation of motility with metastatic potential. Proc Natl Acad Sci U S A 1989;86:1254–8.
23. Nobes CD, Hall A. Rho, rac, and cdc42 GTPases regulate the assembly of multimolecular focal complexes associated with actin stress fibers, lamellipodia, and filopodia. Cell 1995;81:53–62.
24. Wheeler AP, Ridley AJ. Why three Rho proteins? RhoA, RhoB, RhoC, and cell motility. Exp Cell Res 2004;301:43–9.
25. Hakem A, Sanchez-Sweatman O, You-Ten A, Duncan G, Wakeham A, Khokha R, et al. RhoC is dispensable for embryogenesis and tumor initiation but essential for metastasis. Genes Dev 2005;19:1974–9.
26. Nielsen TO, Parker JS, Leung S, Voduc D, Ebbert M, Vickery T, et al. A comparison of PAM50 intrinsic subtyping with immunohistochemistry and clinical prognostic factors in tamoxifen-treated estrogen receptor-positive breast cancer. Clin Cancer Res 2010;16:5222–32.

27. Simon C, Goepfert H, Boyd D. Inhibition of the p38 mitogen-activated protein kinase by SB 203580 blocks PMA-induced Mr 92,000 type IV collagenase secretion and *in vitro* invasion. Cancer Res 1998;58: 1135–9.
28. Chen L, Mayer JA, Krisko TI, Speers CW, Wang T, Hilsenbeck SG, et al. Inhibition of the p38 kinase suppresses the proliferation of human ER-negative breast cancer cells. Cancer Res 2009;69:8853–61.
29. Sabio G, Arthur JS, Kuma Y, Peggie M, Carr J, Murray-Tait V, et al. p38gamma regulates the localisation of SAP97 in the cytoskeleton by modulating its interaction with GKAP. EMBO J 2005;24: 1134–45.
30. Kim JH, Cho A, Yin H, Schafer DA, Mouneimne G, Simpson KJ, et al. Psidin, a conserved protein that regulates protrusion dynamics and cell migration. Genes Dev 2011;25:730–41.
31. Weiner OD, Marganski WA, Wu LF, Altschuler SJ, Kirschner MW. An actin-based wave generator organizes cell motility. PLoS Biol 2007;5: e221.
32. Del Alamo JC, Meili R, Alonso-Latorre B, Rodriguez-Rodriguez J, Aliseda A, Firtel RA, et al. Spatio-temporal analysis of eukaryotic cell motility by improved force cytometry. Proc Natl Acad Sci U S A 2007;104:13343–8.
33. Barnhart EL, Allen GM, Julicher F, Theriot JA. Bipedal locomotion in crawling cells. Biophys J 2010;98:933–42.
34. Cano A, Perez-Moreno MA, Rodrigo I, Locascio A, Blanco MJ, del Barrio MG, et al. The transcription factor snail controls epithelial-mesenchymal transitions by repressing E-cadherin expression. Nat Cell Biol 2000;2:76–83.
35. Yang J, Mani SA, Donaher JL, Ramaswamy S, Itzykson RA, Come C, et al. Twist, a master regulator of morphogenesis, plays an essential role in tumor metastasis. Cell 2004;117:927–39.
36. Chiang AC, Massague J. Molecular basis of metastasis. N Engl J Med 2008;359:2814–23.
37. van Golen KL, Wu ZF, Qiao XT, Bao LW, Merajver SD. RhoC GTPase, a novel transforming oncogene for human mammary epithelial cells that partially recapitulates the inflammatory breast cancer phenotype. Cancer Res 2000;60:5832–8.
38. Wu M, Wu ZF, Merajver SD. Rho proteins and cell-matrix interactions in cancer. Cells Tissues Organs 2007;185:100–3.
39. van Golen KL, Bao LW, Pan Q, Miller FR, Wu ZF, Merajver SD. Mitogen activated protein kinase pathway is involved in RhoC GTPase induced motility, invasion and angiogenesis in inflammatory breast cancer. Clin Exp Metastasis 2002;19:301–11.
40. Clark EA, Golub TR, Lander ES, Hynes RO. Genomic analysis of metastasis reveals an essential role for RhoC. Nature 2000;406: 532–5.
41. Ikoma T, Takahashi T, Nagano S, Li YM, Ohno Y, Ando K, et al. A definitive role of RhoC in metastasis of orthotopic lung cancer in mice. Clin Cancer Res 2004;10:1192–200.
42. Islam M, Lin G, Brenner JC, Pan Q, Merajver SD, Hou Y, et al. RhoC expression and head and neck cancer metastasis. Mol Cancer Res 2009;7:1771–80.
43. Wu M, Wu ZF, Rosenthal DT, Rhee EM, Merajver SD. Characterization of the roles of RhoC and RhoA GTPases in invasion, motility, and matrix adhesion in inflammatory and aggressive breast cancers. Cancer 2010;116:2768–82.
44. Ridley AJ. Rho GTPases and cell migration. J Cell Sci 2001;114: 2713–22.
45. Rosenthal DT, Brenner JC, Merajver SD. Rho proteins in cancer. In: van Golen KL, editor. The Rho GTPases in cancer. New York: Springer New York; 2010. p. 29–42.
46. Li YP, Chen Y, John J, Moylan J, Jin B, Mann DL, et al. TNF-alpha acts via p38 MAPK to stimulate expression of the ubiquitin ligase atrogin1/MAFbx in skeletal muscle. FASEB J 2005;19:362–70.
47. Bellei B, Maresca V, Flori E, Pitisci A, Larue L, Picardo M. p38 regulates pigmentation via proteasomal degradation of tyrosinase. J Biol Chem 2010;285:7288–99.
48. Nethe M, Hordijk PL. The role of ubiquitylation and degradation in RhoGTPase signalling. J Cell Sci 2010;123:4011–8.